Fluid/Structure interaction in open channel using CFD approach

Fouzi BENMOUSSA[1*], Hocine BENMOUSSA[1], Ahmed BENZAOUI[2]

[1] Laboratory (LESEI), Faculty of Technology, Mechanics Department. Hadj Lakhdar University, Batna, Algeria

[2] Laboratory of Thermodynamics and Energy Systems, Faculty of Physics. Houari Boumedienne Sciences and Technology University, Algiers, Algeria

*benmoussa_fouzi@yahoo.fr

Abstract - The present work deals with a numerical study of three-dimensional incompressible free-surface flow in rectilinear channel of rectangular section over a parallelepiped obstacle placed on the channel bottom wall. The finite volume computational fluid dynamics module of the Fluent software was used to solve the continuity and momentum equations. The main objective of the numerical simulation is devoted to examine the three-dimensional structure of the free-surface flow around an obstacle: Three-dimensional visualization of the interaction Fluid/Obstacle, visualization of the recirculation zone, velocity and pressure profiles. The study of the hydrodynamic effects of the obstacle on the flow consists in analyzing these processes in terms of zones of influences (upstream and downstream) in order to examine the three-dimensional structure of the free-surface flow around an obstacle.

Résumé - Le présent travail concerne une étude numérique tridimensionnelle d'un écoulement à surface libre d'un fluide incompressible dans un canal rectiligne de section rectangulaire au-dessus d'un obstacle parallélépipède s'appuyant sur l'une des parois. L'outil d'investigation étant le logiciel Fluent modèle numérique tridimensionnel en volumes finis utilisant les équations de Navier-Stockes. L'objectif principale de cette simulation est consacré à examiner la structure tridimensionnelle de l'écoulement autour d'un obstacle: visualisation tridimensionnelle de l'interaction Écoulement/Obstacle, visualisation de la zone de recirculation, profils de vitesse axiale et profils de pression. L'étude des effets hydrodynamiques de l'obstruction sur l'écoulement consiste à analyser ces processus en termes de zones d'influences (en amont et en aval) afin d'examiner la structure tridimensionnelle de l'écoulement autour de cet obstacle.

Keywords: Free-surface flow, Fluid-Structure interaction, Computational fluid dynamics, Navier-Stokes equation.

Nomenclature

U	Instantaneous velocity, $m.s^{-1}$	*Greek symbols*	
g	Acceleration of gravity, $m.s^{-2}$	ρ	Density of fluid, $Kg.m^{-3}$
P	Pression, Pa	μ	Viscosity of fluid, $Kg.m^{-1}.s^{-1}$
S	Source term	Φ	Transported property
$x,$	Cartesian coordinates	Γ	Coefficient of diffusion, $Kg.m^{-1}.s^{-1}$
		D	Deformation rate, $Kg.m^{-2}.s^{-2}$

1. Introduction

Free-surface flows in the natural environments occur in general with inhomogeneous boundary conditions because of the roughness distribution of the bottom, fixed or mobile and/or the significant deformations of the free-surface in particular when it has an impact with obstacles. The free-surface flows in rectilinear channels, the interaction between the flow and the obstacle are at the origin of secondary currents generated by the anisotropy of turbulence. These secondary currents are organized in cellular moving in a plan perpendicular to the principal direction of the flow, and their speed does not exceed 3 to 5% of the average speed [1]. In parallel, a lot of studies and mathematical models have been carried out to simulate the three-dimensional structure of the free-surface flows around an obstacle of various forms.

Among these studies we quotes those of Lu Lin et al. [2] which proposed a two-dimensional hybrid numerical model, FEM-LES-VOF for free-surface flows, which is a combination of three-step Taylor-Galerkin finite element method, large eddy simulation for turbulence model and computational Lagrangian-Eulerian volume of fluid method. Using the FEM-LES-VOF model, the free-surface flow over a semi-circular obstruction is investigated. The simulation results are compared with available experimental and numerical results. Good performance of the FEM-LES-VOF model is demonstrated. Franc Vigie [3] numerically investigated a free-surface flow over a single two-dimensional obstacle placed on the channel bottom wall. The main objective is to determine the obstacle role and its influence on the flow dynamics. Two obstacles, a semi-cylinder and a flat gaussian one are used in this work. For both obstacles, free-surface profiles in the channel centerline are performed using water depth measurements. These profiles are classified in surface waves regimes, depending on the flow parameters: the Froude number and the blocking factor, which compares the obstacle's height and the undisturbed water depth. Hydrodynamics in the obstacle vicinity is characterized with two-dimensional velocity field measurements. Mean-velocity-field topology and turbulence structure are analysed. Some of physical mechanisms, controlling the free-surface shape and the local structure of the flow, are exhibited.

The main objective of the present paper is devoted to examine the three-dimensional structure of the free-surface flow around a parallelepiped obstacle placed on the channel bottom wall in rectilinear channel of rectangular section: Three-dimensional visualization of the interaction Fluid/Obstacle, visualization of the recirculation zone, velocity and pressure profiles.

2. Physical model and mathematical formulation

We present our physical model, the assumptions, as well as the mathematical formulation which describes the phenomenon of an incompressible flow has free-surface in rectilinear channel.

2.1.Physical model

The physical model studied in this paper is horizontal channel (null slope), with length ($L_{channel}$ = 8 m), and constant rectangular section (Width $l_{channel}$ = 1.2 m, Height $H_{channel}$ = 0.4 m). To study numerically the interaction Fluid/Obstacle, a parallelepiped emerged obstacle (20 mm thickness, 0.2 m height, and 0.4 m width) was oriented perpendicular to the channel side wall to 2.6 m of the exit face of the channel as shown in Figure 1.

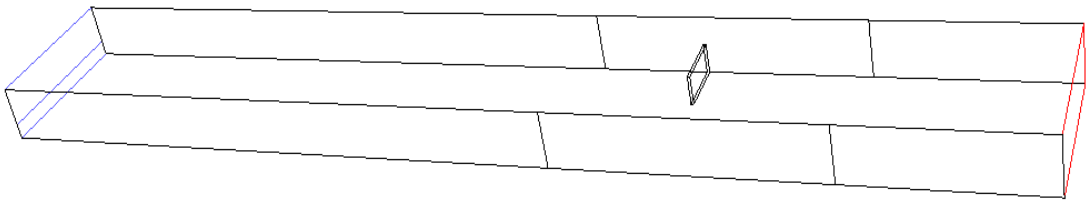

Figure 1. Physical configuration of rectilinear channel with a parallelepiped obstacle placed on the channel bottom wall

2.2.Assumptions

In order to simplify the physical and mathematical model, the following assumptions are adopted.

- The free-surface flow is incompressible and can be considered as a Newtonian fluid;
- Immiscible fluids (no interpenetration between fluids, air and water);
- The centrifugal rotational forces is negligible compared to the gravity force;
- No thermal transfer.

2.3.Governing equations

Mathematical formulation involves the Navier–Stokes equations, which are based on the assumptions of conservation of mass and momentum within a moving fluid. The continuity and momentum equations for incompressible flow may be written in the cartesian tensor notation as follows [4]:

$$\frac{\partial U_i}{\partial x_i} = 0 \tag{1}$$

$$\overbrace{\underbrace{\frac{\partial}{\partial x_j}\left(\rho U_i U_j\right)}_{terme convectif}}^{force d'énercie} = \overbrace{-\underbrace{\frac{\partial P}{\partial x_i}}_{pression} + \underbrace{\mu \frac{\partial^2 U_i}{\partial x_j^2}}_{terme visqueux} + \underbrace{\rho g_i}_{force de gravité}}^{force appliquées} \tag{2}$$

The viscous term can be written according to the deformation rate tensor D_{ij} :

$$\frac{\partial}{\partial x_j}\left(\rho U_i U_j\right) = -\frac{\partial P}{\partial x_i} + \frac{\partial}{\partial x_j}\left[\mu\left(\frac{\partial U_i}{\partial x_j} + \frac{\partial U_j}{\partial x_i}\right)\right] + \rho g_i \tag{3}$$

Calculations of the three-dimensional (3-D) free-surface flow in open channel are based on the solution of the transport equation (of form convection-diffusion) governing the equations of continuity and momentum:

$$\frac{\partial\left(\rho\bar{U}\Phi\right)}{\partial x}+\frac{\partial\left(\rho\bar{V}\Phi\right)}{\partial y}+\frac{\partial\left(\rho\bar{W}\Phi\right)}{\partial z}=\frac{\partial}{\partial x}\left(\Gamma\frac{\partial\Phi}{\partial x}\right)+\frac{\partial}{\partial y}\left(\Gamma\frac{\partial\Phi}{\partial y}\right)+\frac{\partial}{\partial z}\left(\Gamma\frac{\partial\Phi}{\partial z}\right)+S_{\Phi} \quad (4)$$

Where Φ is the transported property, Γ_{Φ} the coefficient of diffusion and S_{Φ} the source term.

The first term of the transport equation called ''Convectif term'', the second term called ''Diffusif term'', and the third term called ''Source term''.

The expressions of the transported property, coefficient of diffusion and source term vary according to the types of equations to be solved. For the continuity equation, the transported property presents the volume fraction, the coefficient of diffusion and the source term are null. For the momentum equation, the transported property presents the instantaneous velocity, the coefficient of diffusion presents the deformation rate tensor, and the source term includes the pressure and gravity term.

3. Resolution and discretisation method

3.1.Grid system and discretisation

The governing equations based on the above assumptions including continuity and momentum equations were reformulated and numerically investigated in (3-D) coordinates, which can describe the phenomenon of an incompressible free-surface flow in rectilinear channel over obstacle. The finite volume method is used to discrete the transport equation. For easy capturing of the discretisation process, the schematic diagram of grid system is shown in Figure 2, 3.

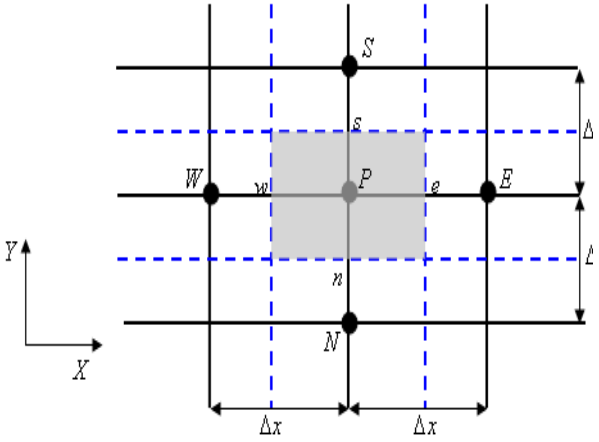

Figure 2: Schematic diagram of grid system in the channel. Vertical plane (X, Y).

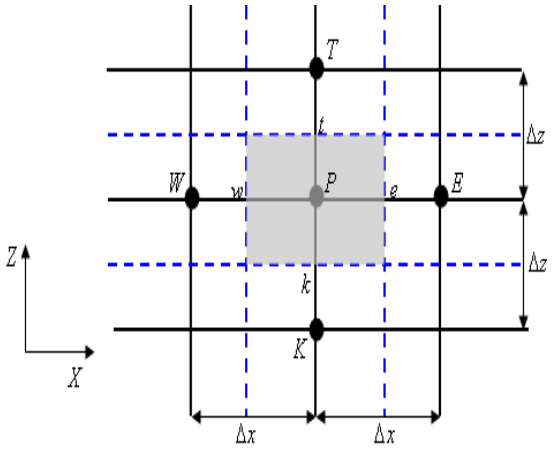

Figure 3: Schematic diagram of grid system in the channel. Horizontal plane (X, Z).

$$\int_k^t\int_n^s\int_w^e\left(\frac{\partial\left(\rho\overline{U}\Phi\right)}{\partial x}+\frac{\partial\left(\rho\overline{V}\Phi\right)}{\partial y}+\frac{\partial\left(\rho\overline{W}\Phi\right)}{\partial z}\right)dx.dy.dz=\int_k^t\int_n^s\int_w^e\left(\frac{\partial}{\partial x}\left(\Gamma\frac{\partial\Phi}{\partial x}\right)+\frac{\partial}{\partial y}\left(\Gamma\frac{\partial\Phi}{\partial y}\right)+\frac{\partial}{\partial z}\left(\Gamma\frac{\partial\Phi}{\partial z}\right)\right)dx.dy.dz$$

$$+\int_k^t\int_n^s\int_w^e S_\Phi dx.dy.dz \qquad (5)$$

Result discretisation of the convectif term

$$\Delta y.\Delta z\left[\left(\rho\overline{U}\Phi\right)_e-\left(\rho\overline{U}\Phi\right)_w\right]+\Delta x.\Delta z\left[\left(\rho\overline{V}\Phi\right)_s-\left(\rho\overline{V}\Phi\right)_n\right]+\Delta x.\Delta y\left[\left(\rho\overline{W}\Phi\right)_t-\left(\rho\overline{W}\Phi\right)_k\right] \qquad (6)$$

Result discretisation of the diffusif term

$$\Delta y.\Delta z\left[\left(\Gamma\frac{\partial\Phi}{\partial x}\right)_e-\left(\Gamma\frac{\partial\Phi}{\partial x}\right)_w\right]+\Delta x.\Delta z\left[\left(\Gamma\frac{\partial\Phi}{\partial y}\right)_s-\left(\Gamma\frac{\partial\Phi}{\partial y}\right)_n\right]+\Delta x.\Delta y\left[\left(\Gamma\frac{\partial\Phi}{\partial z}\right)_t-\left(\Gamma\frac{\partial\Phi}{\partial z}\right)_k\right] \qquad (7)$$

Result discretisation of the source term

$$\int_k^t\int_n^s\int_w^e\overline{S}_\Phi\,dx.dy.dz=\overline{S}_\Phi\Delta x.\Delta y.\Delta z=\left(S_p\Phi_p+S_u\right)\Delta x.\Delta y.\Delta z \qquad (8)$$

The linear form of the transport equation after discretisation of all terms is:

$$a_p\Phi_p=\sum_{nb}a_{nb}\Phi_{nb}+b \qquad (9)$$

Where a_p, a_{nb} are coefficients, *nb: r*epresent the indices of the vicinity cells in the computational grid. Fluent solves this linear system by using an implicit specific solver of linear equations (Gauss-Seidel).

3.2.Computational domain

The computational domains were created in the commercial pre-processor software Gambit. It was also used for meshing, labeling boundary conditions and determines the computational domain.

During generation the computational grid we pass by the following instructions:

- The creation of volume and the definition of its dimensions, Figure 4
- Meshing the faces and volume, Figure 5

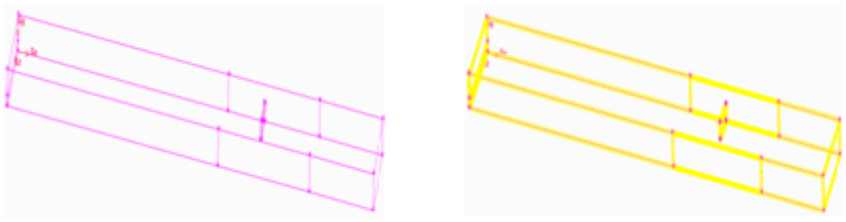

Figure 4: Creation of the geometry in (3-D)

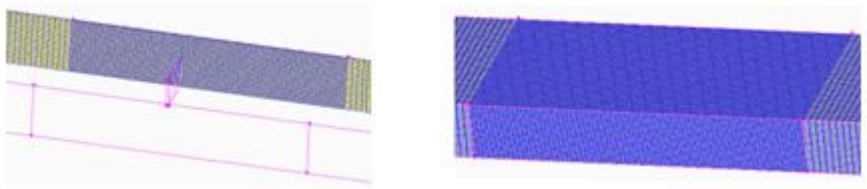

Figure 5: Meshing the vertical face and volume

- The insertion of the boundary conditions on various surfaces of volume, Figure 6

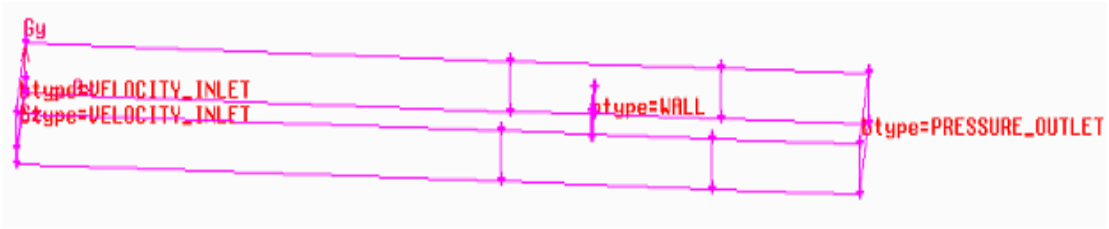

Figure 6: Different types of boundary conditions

3.3.Boundary conditions

Two different velocity inlets were needed to define the water flow (Inlet I) and air flow (Inlet II) in the model domain called *''Velocity-inlet''* function. These inlets were defined as stream-wise velocity inlets that require the values of velocity. For the pressure we used the *''Pressure outlet''* function to define the value of the pressure in the exit face of the channel. Finally to estimate the effect of walls on the flow (roughness distribution), empirical *''Wall''* function was used. Convergence was reached when the normalized residual of each variable (continuity residual, velocity, pressure) was on the order of 1×10^{-3} and the computation for about 450 iterations.

3.4.Two-dimensional examination of the mesh

In the present paper, an unstructured mesh was used in both horizontal and vertical planes around the parallelepiped obstacle, because of the important and rapid variation in the flow characteristics. Figure 7 shows the mesh for the numerical model. The area around the obstacle used a finer mesh than the other region. The number of mesh in horizontal and vertical view was increased near the obstacle to trace more accurately the flow parameters (velocity, pressure …etc). The final number of mesh in various conditions is 241527cells.

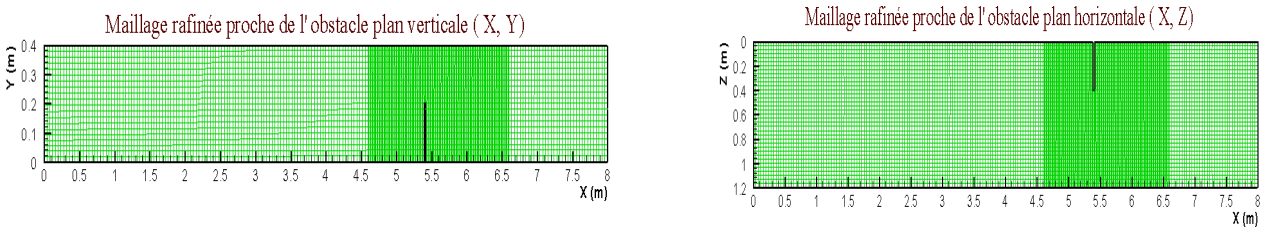

Figure 7: Computational grid in the obstacle vicinity in both horizontal and vertical planes.

4. Analysis of computational results

4.1.Three-dimensional visualization of the interaction Fluid/Obstacle

The interaction between the flow and the obstacle is shown in Figure 8. The presence of the obstacle in the channel creates strong disturbances in the flow, which modified the overall structure of the flow. The following statements can be drawn from the below results:

- Blocking of the flow with formation of a mascaret which propagates upstream and above the obstacle when the flow impact the obstacle (Collisional regime) (Y = 0.05, 0.1, 0.2, 0.25) m.
- A permanent regime can be reached with the formation of a stationary rise (Y = 0.3 m).
- Disappearance of the rise and transition toward the inertial regime and formation a jet with significant length (strong curve of the free-surface over the obstacle) (Y= 0.3 m).

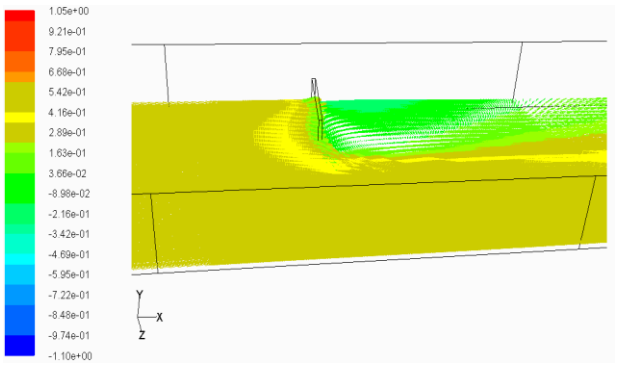

Horizontal plane (Y = 0.05 m)

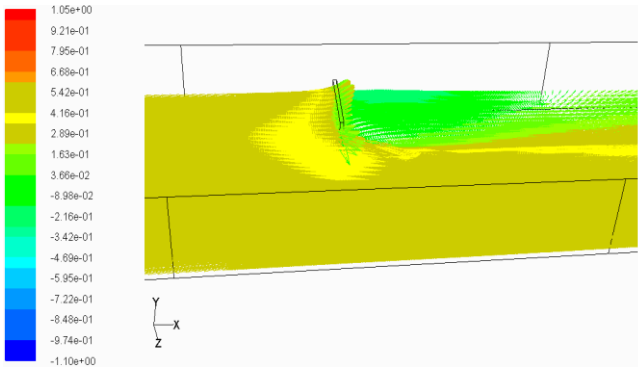

Horizontal plane (Y = 0.1 m)

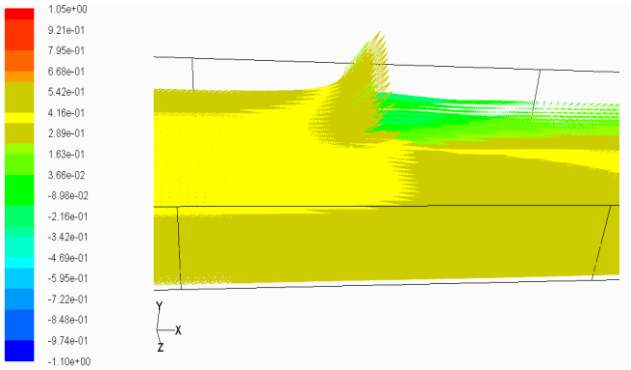

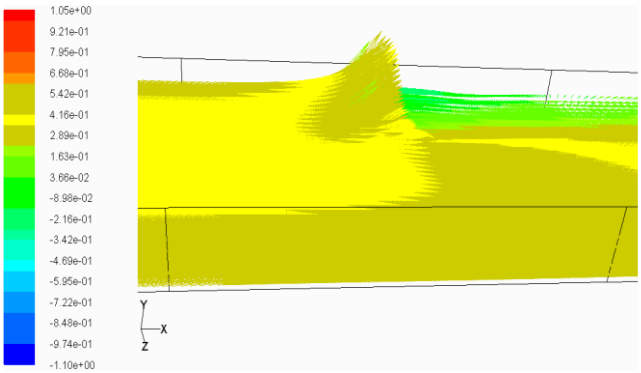

Horizontal plane (Y = 0.2 m)

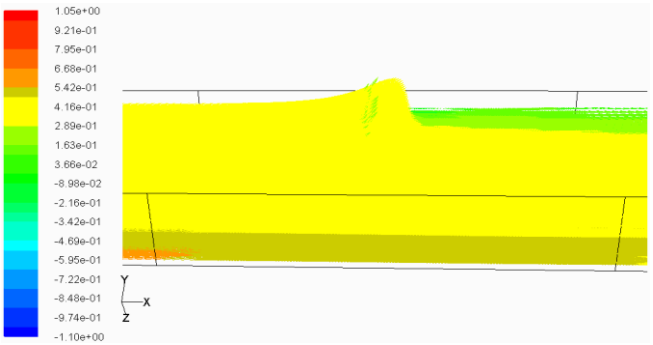

Horizontal plane (Y = 0.25 m)

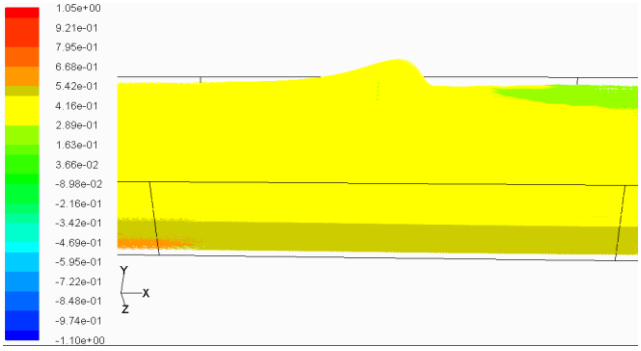

Horizontal plane (Y = 0.3 m)

Horizontal plane (Y = 0.35 m)

Figure 8: Three-dimensional visualization of the interaction Fluid/Obstacle

4.2.Visualization of the recirculation zone

Secondary currents vectors around the obstacle are shown in Figure 9. A recirculation zone formed downstream from the obstacle due to the direction of flow by the obstacle. The recirculation zone shown in Figure 9, in horizontal plane situated near the bottom takes the shape of contrarotating rollers, located in the alignment of the obstacle and extends until the exit of the channel. The flow pattern formed downstream from the obstacle in the present geometry is expected to be very similar to the one observed by other researchers [5, 6].

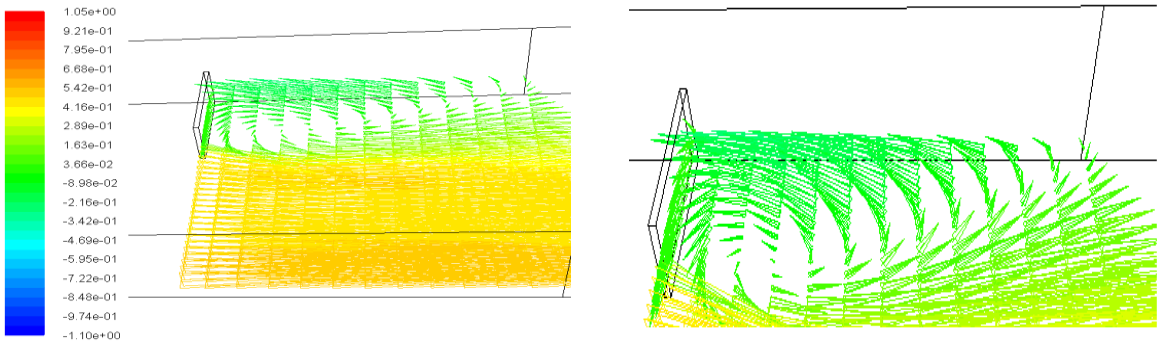

Figure 9: Visualization of the recirculation zone

4.3.Velocity profiles

The axial velocity profiles in both horizontal and vertical planes around the obstacle are shown in Figure 10. The following statements can be drawn from the below results:

- It's observed for each vertical plane the significant velocity variation with the variation of the horizontal station Y (Flow level).

- The flow reaches the obstacle with significant velocity dropping (0.4 m/s), (long distance between the flow inlet and obstacle position 5.4 m), (Z= 0.1, 0.2, 0.3, 0.4) m.
- Downstream of the obstacle, the recirculation region appears well behind the obstacle (velocity presented by negative values), especially for the two planes (Z= 0.1, 0.2) m, which present the corner region in the channel. The extremity of the obstacle presents less recirculation.
- Because of the reduction in the passage section of the flow, we can notice an acceleration in velocity between space wall-obstacle (Z= 0.6, 0.8) m.

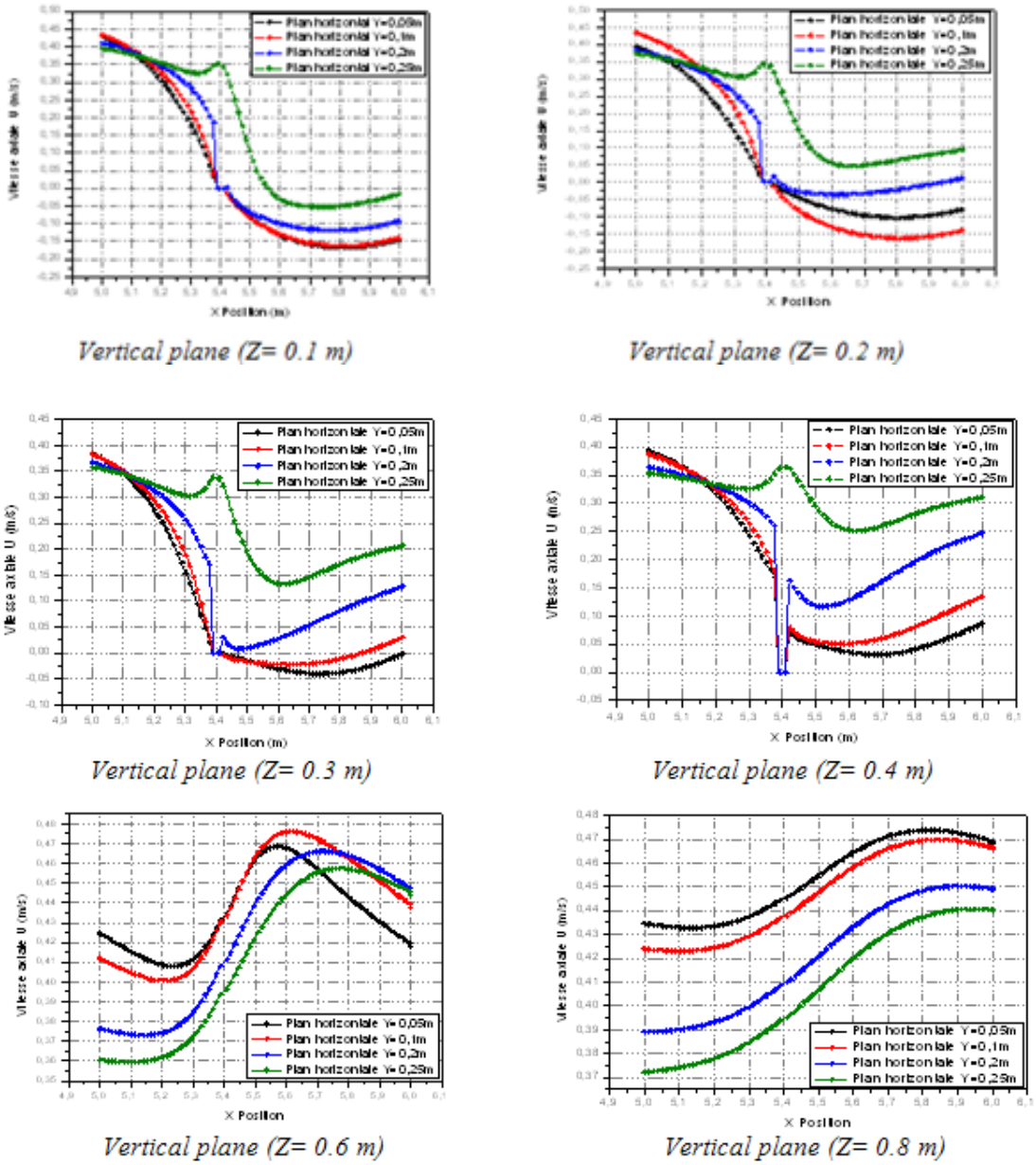

Figure 10: Axial velocity profiles U (m/s) in different vertical planes around the obstacle

4.4.Pressure profiles

The axial pressure profiles upstream and downstream from the obstacle in both horizontal and vertical planes are shown in Figure 11. The following statements can be drawn from the below results:

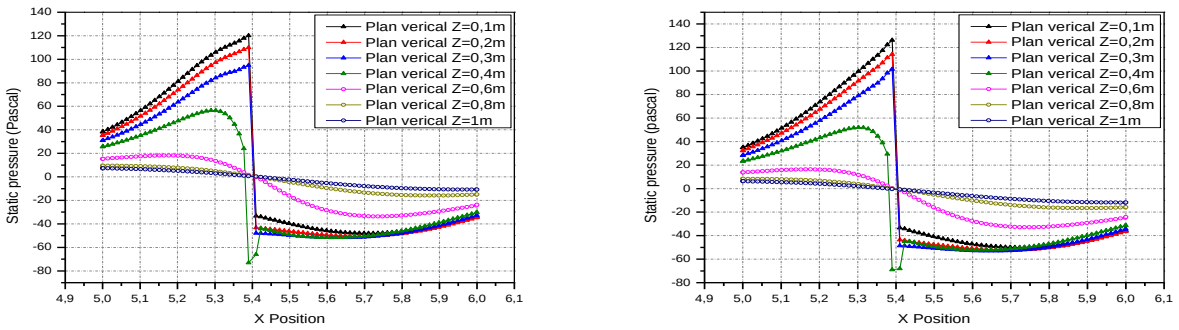

Horizontal plane (Y= 0.05 m) *Horizontal plane (Y= 0.1 m)*

Figure 11: Axial pressure profiles in different horizontal planes around the obstacle

- The evolution of pressure in the channel undergone a jump on the obstacle, the increase in pressure reaches a maximum value when the flow impact the obstacle (Collisional regime), the maximum value was located in (Z= 0.1 m), which present the corner region of the channel. More we move away from the corner region to the extremity of the obstacle, the increasing becomes weak.
- Downstream from the obstacle, the pressure profiles shows a significant dropping (Recirculation zone).

5. Conclusion

In this research, free-surface flow around a parallelepiped obstacle in rectilinear channel of rectangular section was studied using a (3-D) numerical hydraulic model. The finite volume computational fluid dynamics module of the Fluent software was used to solve the transport equations (of form convection-diffusion) governing the equations of continuity and momentum in order to simulate the main characteristics of the free-surface flow around obstacle. By comparing the (3-D) model with the others results in the literature, the model was found to produce flow around a parallelepiped obstacle with sufficient accuracy. The study of the hydrodynamic effects of the obstacle on the flow consists in analyzing these processes in terms of zones of influences (upstream and downstream) in order to examine the three-dimensional structure of the free-surface flow around an obstacle.

References

1. C. Labiod. Ecoulement a surface libre sur fond de rugosité inhomogène. Thèse présenté pour obtenir le titre de docteur de l'université de Toulouse. Spécialité : Sciences de la Terre et de l'Environnement. N° d'ordre: 2242.

2. L. Lin, L. Yu-Cheng, T. Bin. Numerical simulation of turbulent free surface flow over obstruction. Journal of Hydrodynamics. 20 (2008) 414-423.

3. F. Vigie. Etude expérimentale d'un écoulement à surface libre au-dessus d'un obstacle. Thèse présenté pour obtenir le titre de docteur de l'université de Toulouse. Spécialité: Energétique et Dynamique des Fluides. No d'ordre: 2258.

4. W. Czernuszenko, A. Rylov. Modeling of three-dimensional velocity field in open channel flows. Journal of Hydraulic Research. 40(2002) 135-143.

5. J. Yazdi, H. Sarkardeh, H. Azamathulla, A. Ghani. 3D simulation of flow around a single spur dike with free-surface flow. International Journal of River Basin Management. 8 (2010) 55-62.

6. M. Andrew, C. George, W. Larry. Exchange processes in a channel with two vertical emerged obstructions. Springer Science+Business Media B.V. 2006